



Investigation of Li/Ca variations in aragonitic shells of the ocean quahog *Arctica islandica* (northeast Iceland)

Julien Thébault ^{a,*}, Bernd R. Schöne ^a, Nadine Hallmann ^a, Matthias Barth ^b, and Elizabeth V. Nunn ^a

^a Earth System Science Research Centre (Geocycles), Department of Applied and Analytical Paleontology (INCREMENTS), Institute of Geosciences, University of Mainz, Johann-Joachim-Becherweg 21, 55128 Mainz, Germany

^b Earth System Science Research Centre (Geocycles), Department of Geochemical Petrology, Institute of Geosciences, University of Mainz, Johann-Joachim-Becherweg 21, 55128 Mainz, Germany

Running title: Li/Ca record in aragonitic bivalve shells

* Correspondence author. Present address: Université de Bretagne Occidentale, Laboratoire des Sciences de l'Environnement Marin (UMR6539 UBO/CNRS/IRD), Institut Universitaire Européen de la Mer, Technopole Brest-Iroise, Place Nicolas Copernic, 29280 Plouzané, France. Phone: +33 2 98 49 86 33; Fax: +33 2 98 49 86 45; Email: julien.thebault@univ-brest.fr

1
2
3 **ABSTRACT**

4 Inter- and intra-annual variations in lithium-to-calcium ratio were investigated with high
5 temporal resolution in the aragonitic outer shell layer of juvenile *Arctica islandica* (Mollusca;
6 Bivalvia) collected alive in 2006 off northeast Iceland. $\text{Li}/\text{Ca}_{\text{shell}}$ ranged between 7.00 and
7 $11.12 \mu\text{mol mol}^{-1}$ and presented well-marked seasonal cycles with minimum values recorded
8 at the annual growth lines; a general pattern was a progressive increase in $\text{Li}/\text{Ca}_{\text{shell}}$ from
9 March to May, followed by a plateau in June, and a decrease down to minimum values in
10 July–August. $\text{Li}/\text{Ca}_{\text{shell}}$ was correlated with $\delta^{18}\text{O}_{\text{shell}}$ -derived temperature but the strength of
11 this relationship was weak ($r^2 < 0.25$; $p < 0.05$). It covaried significantly with microgrowth
12 increment width and with the discharge from one of the closest rivers. Seasonal variations of
13 $\text{Li}/\text{Ca}_{\text{shell}}$ in *A. islandica* may most likely be explained (1) by calcification rate, and/or (2) by
14 significant river inputs of Li-rich silicate particles flowing to the sea as soon as snow melts. In
15 the first case, $\text{Li}/\text{Ca}_{\text{shell}}$ may be a useful proxy for addressing seasonal variations of growth
16 rate in bivalves that lack discernable microgrowth patterns. Abrupt decreases of $\text{Li}/\text{Ca}_{\text{shell}}$ may
17 in turn help identify growth retardations due to harsh environmental conditions. Alternatively,
18 if $\text{Li}/\text{Ca}_{\text{shell}}$ variations are linked to particulate Li inputs by rivers, this could be a new proxy
19 for the intensity of mechanical weathering of Icelandic basalts, with interesting perspectives
20 for the reconstruction of frequency and intensity of past jökulhlaups (subglacial outburst
floods). Further works, including experimental studies, are needed to test these hypotheses.

21 **Keywords:** bivalve; lithium; calcification; shell growth rate; weathering; Iceland

22 **Index Terms:**

23 0424 Biogeosciences: Biosignatures and proxies

24 0438 Biogeosciences: Diel, seasonal, and annual cycles (4227)

25 0454 Biogeosciences: Isotopic composition and chemistry (1041, 4870)

26 4870 Oceanography: Biological and chemical: Stable isotopes (0454, 1041)

27 4875 Oceanography: Biological and chemical: Trace elements (0489)

28
29
30
31
32
33
34
35
36
37
38
39
40
41
42
43
44
45
46
47
48
49
50
51
52

1. INTRODUCTION

During the past sixty years, a large number of studies have focused on the use of elemental concentrations in marine sediment cores as proxies for past variations of environmental parameters. These parameters include, among others, temperature (proxies: Mg/Ca, Sr/Ca), alkalinity (Ba/Ca), dissolved inorganic carbon concentration (Cd/Ca), ocean circulation (Cd/Ca, Nd, Hf, Pb), biological productivity (BaSO₄, Pa/Th, Be/Th, U) and sedimentation rate (²³⁰Th, ²¹⁰Pb, ²³¹Pa/²³⁰Th) (for thorough reviews, see: Wefer et al., 1999; Henderson, 2002). However, the temporal resolution of such paleoceanographic reconstructions is low, generally coarser than decades. Therefore, efforts have been made to assess the potential of elemental content in marine biogenic carbonates, especially bivalve mollusk shells, as high-resolution proxies for environmental conditions (e.g. Stecher et al., 1996; Vander Putten et al., 2000; Thébault et al., 2009).

Bivalve shells grow by accretion of calcium carbonate crystals, either in the form of calcite, aragonite, or both depending on the species (Pannella and MacClintock, 1968). Shell growth, however, does not occur continuously over a day, or over a year; instead, growth ceases periodically, on ultradian (several growth stops during a single day), circatidal (semi-diurnal, ca. 12.4h), circadian (solar day, ca. 24h), circalunidian (lunar day, ca. 24.8h), or annual timescales (Schöne, 2008). These growth stops result in the formation of so-called growth lines, which are enriched in organic matter and separate growth increments that represent equal time slices. These periodic growth lines can therefore be used to assign precise calendar dates to each successive increment of accreted shell material. This characteristic gives bivalve shells an outstanding potential for the high-resolution reconstruction of paleoenvironmental conditions, especially through geochemical analyses. For example, skeletal oxygen isotope composition ($\delta^{18}\text{O}$) of many bivalve species (including

53 scallops, mussels, and clams) has been extensively used since the pioneering work of Epstein
54 et al. (1953) to infer paleotemperature variations, sometimes with an accuracy of less than
55 1°C (Chauvaud et al., 2005; Thébault et al., 2007).

56 In the past decade, the elemental composition of bivalve shells has also been
57 increasingly used for paleoenvironmental reconstructions. Bivalve shells are not exclusively
58 made of CaCO₃. Aside from Ca, a number of minor and trace elements are also incorporated
59 within the shell during its formation, either in an interstitial location within the crystal lattice
60 or as carbonates (substitution for Ca²⁺; Okumura and Kitano, 1986), or even within the
61 organic matrix (Lingard et al., 1992), which can represent up to 5% of the shell dry weight
62 (Marin and Luquet, 2004). The incorporation of these elements is known to be partly
63 controlled by various environmental parameters, either physical (temperature, salinity),
64 chemical (seawater elemental concentration, metallic contamination), or biological (primary
65 production). Physiology, however, also exerts an important control on the chemical
66 composition of bivalve shells (Schöne, 2008).

67 Micro-analytical techniques (e.g. laser ablation coupled to an ICP-MS system = LA-
68 ICP-MS; Craig et al., 2000) allow the accurate measurement of tens of elements archived in
69 biogenic carbonates within a few seconds. Their abiding improvement considerably increases
70 the probability of discovering new paleoenvironmental proxies. With the exception of a few
71 studies (e.g. Lindh et al., 1988; Carriker et al., 1996; Dick et al., 2007) however, most
72 investigations on the geochemical composition of bivalve shells have only dealt with a few
73 elements (mainly Sr, Mg, Ba, and some trace metals including Mn, Pb, Zn, and Cd).

74 Lithium is a trace element that (1) is easily measurable using mass spectrometers, (2)
75 has been demonstrated to present an interesting potential as a paleoceanographic proxy in
76 some marine biogenic carbonates (Delaney et al., 1985; Delaney et al., 1989; Hall and Chan,
77 2004; Marriott et al., 2004a,b; Hathorne and James, 2006; Montagna et al., 2006), and (3) has

78 surprisingly not yet been analyzed in bivalve shells. One of the first studies dealing with
79 Li/Ca ratios in marine biogenic carbonates suggested that this ratio in foraminiferal calcite
80 was partly controlled by the Li/Ca ratio of the growing medium (Delaney et al., 1985). This
81 was later confirmed by Hathorne and James (2006) who demonstrated that Li/Ca in
82 foraminifera could be used to reconstruct past changes in the Li/Ca ratio of seawater, which
83 could be interpreted in terms of continental silicate weathering rate. Several studies have also
84 highlighted significant inverse relationships between temperature and Li/Ca in foraminifera
85 (Hall and Chan, 2004; Marriott et al., 2004a), in calcitic brachiopods (Delaney et al., 1989), in
86 coralline aragonite (Marriott et al., 2004b; Montagna et al., 2006), and in inorganic calcite
87 (Marriott et al., 2004b). It has finally been suggested that the main factor controlling Li
88 incorporation in foraminifera is not temperature but calcification rate (Hall and Chan, 2004;
89 Marriott et al., 2004a). Because calcification rate may be a function of CO_3^{2-} concentration in
90 the oceans, it has been suggested that the Li/Ca ratio in foraminifera could be a potential
91 proxy of past atmospheric CO_2 (Hall and Chan, 2004).

92 Here, we present for the first time Li/Ca records in bivalve mollusk shells. We have
93 focused on juvenile ocean quahogs *Arctica islandica* (Linnaeus, 1767) collected alive in 2006
94 off the coast of northeast Iceland, probably one of the last pristine ecosystems in the North
95 Atlantic. *A. islandica* has all the characteristics necessary for paleoceanographic
96 reconstructions. First, it produces circadian and annual growth patterns in its aragonitic shell
97 (Schöne et al., 2005a). Second, it holds the longevity record for bivalves and may in fact be
98 the longest-lived non-colonial animal, living up to 4 centuries (Schöne et al., 2005b;
99 Wanamaker et al., 2008a). Third, it exhibits a broad biogeographic distribution centered
100 around Iceland, inhabiting the continental shelves on both sides of the North Atlantic, in
101 Europe from the Barents Sea to the Bay of Cadiz in Spain, and in North America from
102 Newfoundland to Cape Hatteras (Thorarinsdóttir and Jacobson, 2005). Fourth, this species has

103 been intensively studied for its anatomy, behavior, physiology, biology, and ecology
104 (Witbaard, 1997). And finally, several studies have already highlighted that shells of
105 *A. islandica* provide multi-proxy records of environmental variables. Changes in
106 environmental parameters are recorded in variations of growth rates (Marchitto et al., 2000;
107 Schöne et al., 2003; Schöne et al., 2005b), stable isotope composition (Weidman et al., 1994;
108 Schöne et al., 2004; Schöne et al., 2005a,b,c; Wanamaker et al., 2008b) and trace element
109 concentrations (Epplé, 2004; Toland et al., 2000; Liehr et al., 2005).

110 The aims of this paper are (1) to analyze the behavior of Li/Ca in *A. islandica* aragonitic
111 shells (inter- and intra-annual variability) using variations of the oxygen isotope composition
112 of these shells as chronological checks, (2) to review the different processes that may explain
113 the temporal variations of this ratio, and (3) to assess if Li/Ca could be a promising addition to
114 the arsenal of proxies already used in bivalve shells.

116 2. MATERIAL AND METHODS

118 2.1. Study area

119 Our study site is located in Þistilfjörður (northeast Iceland; 66°10.751'N –
120 15°21.296'W), 1 km off the southwestern edge of Langanes Peninsula and 3 km away from
121 Hafalónsá estuary (Fig. 1). Hafalónsá and Sandá are the two main rivers flowing into
122 Þistilfjörður. Catchments of these two non-glacial rivers are comprised of old basaltic rocks
123 (> 3.1 million years of age). Water depth at our study site is 30 m and the substrate mainly
124 consists of sand and silt sediments. Hydrographic conditions off north Iceland largely depend
125 on the physical characteristics of the East Icelandic Current, which in turn depend on the
126 eastward transport of Greenland Polar Water by the East Greenland Current and the
127 northward transport of Irminger Atlantic Water by the North Irminger Current (Hopkins,

128 1991). No environmental survey has ever been conducted in Þistilfjörður because of its
129 isolated situation in this remote part of Iceland. The closest site where environmental data are
130 available is located 50 km northeastward of our study site, off the northeastern part of the
131 Langanes Peninsula (Langanes Austur LA1, 66°22'N – 14°22'W; Fig. 1). Environmental
132 conditions at LA1 are also mainly controlled by the relative intensities of the East Icelandic
133 Current and the North Irminger Current. Temperature and salinity are measured at this
134 location at a depth of 20 m by the Oceanographic Group of the Marine Research Institute of
135 Reykjavik using a CTD profiler (data available at <http://www.hafro.is/Sjora/>). This dataset
136 indicates that water temperature is lowest in February–March (mean [2000-2006] = 2.8°C; σ
137 = 0.9°C) and reaches a maximum in August (7.9°C; σ = 0.8°C). Over the same period, salinity
138 variations ranged between 34.4 and 34.8. These temperature and salinity values are similar to
139 those measured at 20-30 m water-depth in two other fjords in North Iceland: Reykjarfjörður
140 (Andrews et al., 2001) and Ísafjörður (Assthorsson, 1990). From early May to the end of
141 August, somewhat lower salinities (< 34) can be observed near the surface in Icelandic fjords
142 because of meltwater runoff from the land. However, these low salinities are restricted to the
143 top 10 m of the water column (Assthorsson, 1990; Andrews et al., 2001). Therefore,
144 temperature and salinity data measured at 20 m depth at LA1 likely reflect those of our study
145 site at 30 m depth.

146 The seawater oxygen isotope composition of our study site was measured on 17th
147 August 2006 ($\delta^{18}\text{O}_{\text{water}} = -0.58 \text{ ‰ VSMOW}$; Salinity = 34.58). Seasonal variations in
148 $\delta^{18}\text{O}_{\text{water}}$ are expected given the salinity variations around the Langanes Peninsula but
149 coefficients of the local $\delta^{18}\text{O}_{\text{water}}$ –salinity relationship are unknown. The $\delta^{18}\text{O}_{\text{water}}$ and salinity
150 values were measured off northwest Iceland in October 1998 (65.98–68.72°N; 22.98–
151 29.25°W; depth = 10-30 m) in the framework of the VEINS Program (Variability of
152 Exchanges In the Northern Seas; data compiled by Schmidt et al., 1999). These data indicate

153 that, over the salinity range 32-35, we can expect a lowering of the $\delta^{18}\text{O}_{\text{water}}$ values of 0.68 ‰
154 for every unit decrease in salinity. Given (1) $\delta^{18}\text{O}_{\text{water}}$ and salinity values measured on
155 17/08/2006 at our study site, and (2) the slope of the $\delta^{18}\text{O}_{\text{water}}$ –salinity relationship derived
156 from the VEINS Program, we can expect seasonal variations of $\delta^{18}\text{O}_{\text{water}}$ at our study site of
157 between – 0.7 and – 0.4 ‰ VSMOW over the salinity range 34.4-34.8.

158

159 **2.2. Shell sampling and preparation**

160 Two specimens of *Arctica islandica* were collected alive on 17 August 2006 by
161 dredging on our study site in Þistilfjörður, at a depth of 30 m. Both specimens (ICE06-6.2-
162 A55 and ICE06-6.2-A56, hereafter simply named A55 and A56) were juveniles with a shell
163 height of 33.0 and 31.2 mm, respectively (shell length of 40.0 and 37.4 mm, respectively; Fig.
164 2a). We chose young specimens because *A. islandica* grows fairly rapidly during early
165 ontogenetic stages (Jones, 1983; Weidman et al., 1994; Jones, 1998; Kilada et al., 2007) and
166 young shells therefore provide the highest temporal resolution in carbonate records.

167 Immediately after dredging, the soft parts were discarded and the right and left valves
168 kept frozen until analysis. The left valves of shells A55 and A56 were gently rinsed with de-
169 ionized water and air-dried. Each valve was mounted on a Plexiglas cube using a two-part
170 methacrylat glue (plastic welder, Gluetec GmbH & Co. KG, Germany) and embedded in a
171 two-part metal-epoxy resin (Wiko, Germany) to strengthen the shell and to avoid shell
172 fracture during sawing (Fig. 2b). Two immediately adjacent, 2.6-mm-thick sections were cut
173 from each valve perpendicular to the growth lines along the axis of maximum growth using a
174 low-speed precision saw (Isomet 1000, Buehler Ltd., IL, USA) equipped with a 0.4 mm thick
175 diamond-coated blade cooled and kept wet using de-ionized water (Fig. 2c). These
176 “mirroring” sections were then mounted on glass slides, manually ground with ca. 12 μm and
177 8 μm SiC powder, and polished with 1 μm Al_2O_3 powder to visualize the internal growth

178 patterns. Thick sections were ultrasonically rinsed with de-ionized water between each
179 grinding/polishing step to remove any adhering grinding powder. Thick section “A” was used
180 for isotopic analyses and thick section “B” for trace elemental analyses. Once geochemical
181 analyses were done, these thick sections were cleaned with ethanol before being etched in the
182 so-called Mutvei’s solution for 25 minutes at 37-40°C in order to resolve inter- and intra-
183 annual growth lines and increments (see Schöne et al. (2005d) for a detailed description of
184 this method). Finally, the sections were gently rinsed with de-ionized water and air-dried.
185 Microgrowth increment width was subsequently measured using the image analysis software
186 Panopea (© 2004 Peinl and Schöne). High-resolution photographs of these four sections were
187 taken using a Nikon Coolpix 995 digital camera attached to a Wild Heerbrugg M3Z
188 stereozoom microscope. Photo stitching software (Photoshop Elements 2.0) was then used to
189 assemble the 25-30 photographs taken for each section into a single, high-resolution picture.

190

191 **2.3. Isotopic analyses**

192 The oxygen isotope ratio ($^{18}\text{O}/^{16}\text{O}$) of marine biogenic carbonate is controlled by
193 temperature and the oxygen isotope composition of the seawater from which it precipitates
194 (McCrea, 1950; Epstein et al., 1953). Therefore, shells of our two *A. islandica* specimens
195 were sampled for isotopic analyses in order to reconstruct variations in the bottom-water
196 temperatures these animals experienced during their life. Aragonite samples (48 and 50
197 samples on shells A55 and A56 respectively) were collected in thick sections “A” using a
198 micro-drill (Minimo C121, Minitor Co. Ltd., Japan) equipped with a 0.3 mm tungsten carbide
199 drill bit (model H52.104.003, Gebr. Brasseler GmbH & Co. KG, Germany). Samples were
200 taken in the outer shell layer along an axis running from the ventral margin and toward the
201 youth portions of the shells. Holes drilled in these sections were ca. 350 μm in diameter.
202 Aliquots of shell aragonite weighing between 38 and 125 μg (mean = 80 μg) were analyzed at

203 the University of Frankfurt using an automated Gas Bench II carbonate device interfaced with
204 a Thermo Finnigan MAT 253 isotope ratio mass spectrometer. Shell isotopic data are
205 expressed in conventional delta (δ) notation (Epstein et al., 1953) relative to the VPDB
206 standard. The in-house standard used was a Carrara marble ($\delta^{18}\text{O}_{\text{Carrara}} = -1.74 \text{ ‰ VPDB}$)
207 calibrated against NBS19. The isotopic value used for this calibration was $\delta^{18}\text{O}_{\text{NBS19}} = -2.20$
208 ‰ VPDB (for more details, see Fiebig et al., 2005). Repeated analyses of this standard
209 yielded a reproducibility (1σ) of 0.07 ‰ VPDB .

210 To temporally align aragonite samples taken between two annual growth lines, we
211 compared the temperature reconstructed from our $\delta^{18}\text{O}_{\text{shell}}$ records (hereafter referred as $T_{\delta^{18}\text{O}}$)
212 with seasonal variations of seawater temperature measured at 20 m depth at station LA1. To
213 this end, we used the empirically determined paleothermometry equation of Grossman and Ku
214 (1986; equation 1 in their paper). A modification of this equation was, however, required as
215 their water values were reported in VSMOW minus 0.27 ‰ (Hut, 1987). Once corrected, their
216 equation translates to:

$$T_{\delta^{18}\text{O}} = 19.43 - 4.34 (\delta^{18}\text{O}_{\text{shell}} - \delta^{18}\text{O}_{\text{water}}) \quad (\text{Eq. 1})$$

217
218
219
220 where $T_{\delta^{18}\text{O}}$ is seawater temperature (in $^{\circ}\text{C}$) reconstructed from $\delta^{18}\text{O}_{\text{shell}}$, and $\delta^{18}\text{O}_{\text{shell}}$ and
221 $\delta^{18}\text{O}_{\text{water}}$ are the oxygen isotope composition of aragonite and water expressed in ‰ relative to
222 the VPDB and VSMOW standards respectively. We used an average $\delta^{18}\text{O}_{\text{water}}$ value of -0.55
223 ‰ VSMOW . In order to estimate the uncertainty on $T_{\delta^{18}\text{O}}$, i.e. half the difference between
224 upper and lower bounds, we applied the following formula using (1) the uncertainty in
225 $\delta^{18}\text{O}_{\text{shell}}$ value given by IR-MS ($\epsilon_{\text{IRMS}} = \pm 0.07 \text{ ‰}$), and (2) the estimated range of $\delta^{18}\text{O}_{\text{water}}$
226 (min. = -0.7 ‰ ; max. = -0.4 ‰):

227

228
$$\text{Uncertainty} = 4.34 \times (2 \epsilon_{\text{IRMS}} + \delta^{18}\text{O}_{\text{water max.}} - \delta^{18}\text{O}_{\text{water min.}}) / 2 \quad (\text{Eq. 2})$$

229

230 This resulted in an absolute uncertainty on $T_{\delta^{18}\text{O}}$ of $\pm 0.95^\circ\text{C}$.

231

232 **2.4. Li/Ca_{shell} analyses**

233 Li/Ca ratios were analyzed in thick sections “B” using LA-ICP-MS at the University of
234 Mainz. An Agilent 7500ce quadrupole ICP-MS (Agilent Technologies Inc., CA, USA)
235 coupled to a UP-213 laser ablation system (New Wave Research, CA, USA) was used with
236 the parameters listed in Table 1. Aragonite samples ($n = 332$ in each shell) were ablated in the
237 outer shell layer from the ventral margin toward the youth portions of the shells at a constant
238 distance from the shell surface (400 μm). The diameter of the laser spots was 80 μm and the
239 distance between the centers of two successive spots was 100 μm (i.e. 20 μm between edges
240 of two successive spots). During acquisition, signal intensities were recorded for ^7Li , ^{43}Ca and
241 ^{44}Ca . The intensity of the isotope of interest was systematically normalized against the ^{43}Ca
242 signal (internal standard) in order to correct for laser beam energy drift, focus variation at the
243 sample surface, and ICP-MS detection drift (see Pearce et al., 1997). The glass reference
244 material NIST SRM 612 was used as a calibration standard with the values of Pearce et al.
245 (1997). Precision (degree of reproducibility) and accuracy (degree of veracity) of the applied
246 method were controlled by repeated analyses of the glass reference material NIST SRM 614
247 (Li concentration value taken from Kurosawa et al., 2002). For each shell, the sequence of
248 analyses was as follows: (NIST612)_{×2} + shell_{×2} + (shell_{×15} + NIST614 + shell_{×15} +
249 NIST612)_{×11} + NIST612. Data processing (including instrumental drift correction and
250 normalization) was performed using GLITTER v.4 software (Macquarie Research Ltd.,
251 Australia; Van Achterbergh et al., 2001), following the methods of Longerich et al. (1996).

252 Li/Ca detection limit at the 99% confidence level was calculated by GLITTER using
253 Poisson counting statistics and was $0.243 \mu\text{mol mol}^{-1}$. Repeated measurements of NIST SRM
254 614 ($n = 22$) yielded a precision of 1.9 % (% RSD). Accuracy was extremely good with a Li
255 concentration value in NIST SRM 614 of $1.687 \pm 0.007 \mu\text{g g}^{-1}$ compared with the
256 recommended value of $1.69 \pm 0.026 \mu\text{g g}^{-1}$ (means \pm standard errors).

257

258 **2.5. Statistical analyses**

259 Two different statistical tests were used to compare the means of two independent
260 samples: Student's *t*-test (large samples: $\min(n_1, n_2) \geq 30$) and Mann-Whitney *U*-test (small
261 samples: $\min(n_1, n_2) < 30$). An analysis of covariance (ANCOVA; $\alpha = 0.05$) was used to test
262 whether there were significant differences between the slopes of the least-square linear
263 regressions ($\text{Li/Ca}_{\text{shell}}$ vs. $T_{\delta^{18}\text{O}}$) calculated for each of the two shells. Homogeneity of residual
264 variances was tested with Bartlett's test ($\alpha = 0.01$). No data were excluded. All statistical
265 analyses were performed according to Scherrer (1984).

266

267

3. RESULTS

268

269 **3.1. $\delta^{18}\text{O}_{\text{shell}}$ profiles**

270 In each shell, $\delta^{18}\text{O}_{\text{shell}}$ profile showed cyclical oscillations in phase with the main growth
271 lines that were revealed after the immersion of shell sections in Mutvei's solution (Fig. 3).
272 This confirms the annual periodicity of these growth lines. Seven main growth lines were
273 observed in both shells, suggesting that both specimens settled on the seafloor in 1999.
274 Isotopic data covered four full years of growth (2002-2005) and the beginning of year 2006.

275 $\delta^{18}\text{O}_{\text{shell}}$ values ranged from 1.64 to 3.51 ‰ in shell A55 and from 1.73 to 3.45 ‰ in
276 shell A56. Annual minima ranged from 1.64 to 2.15 ‰, whereas annual maxima varied

277 between 2.92 and 3.51 ‰ (Table 2). Seasonal $\delta^{18}\text{O}_{\text{shell}}$ cycles were strongly right-skewed with
278 minimum/maximum values occurring shortly before/after the annual growth lines (Fig. 3).

279 These $\delta^{18}\text{O}_{\text{shell}}$ values were converted into temperature ($T_{\delta^{18}\text{O}}$) using Eq. (1) and a
280 $\delta^{18}\text{O}_{\text{water}}$ value of -0.55 ‰ (Fig. 3). Annual minimum temperatures recorded by the shells
281 ranged from 1.8 to 4.4°C (mean [2002-2006] = 3.1°C; $\sigma = 1.0$ °C; Table 2). Mean annual
282 minima in shells A55 (3.0°C) and A56 (3.3°C) were not significantly different from each
283 other (Mann-Whitney $U = 8.5$, $n_1 = n_2 = 5$, $p > 0.05$). Annual maximum temperatures
284 recorded by the shells ranged from 7.7 to 9.9°C (mean [2002-2005] = 8.5°C; $\sigma = 0.8$ °C; Table
285 2). Mean annual maxima in shells A55 (8.4°C) and A56 (8.7°C) did not differ significantly
286 (Mann-Whitney $U = 5$, $n_1 = n_2 = 4$, $p > 0.05$).

287 The offsets between $T_{\delta^{18}\text{O}}$ and T_{LA1} (0.3°C and 0.6°C for average annual minima and
288 maxima respectively) are within the ± 0.95 °C uncertainty on $T_{\delta^{18}\text{O}}$, so it is reasonable to
289 assume that the whole annual range of seawater temperature was recorded by the shells.

290

291 3.2. Li/Ca_{shell} profiles

292 For both specimens, Li/Ca_{shell} profiles showed cyclical variations with minimum values
293 recorded exactly at the annual growth lines (Fig. 3). A general tendency of the seasonal
294 Li/Ca_{shell} variations was a progressive increase after the annual line, followed by a plateau and
295 then a decrease down to minimum values. Maximum Li/Ca_{shell} values tended to occur earlier
296 during the growing season than $\delta^{18}\text{O}_{\text{shell}}$ minima (i.e. before temperature maxima; Fig. 3).

297 Li/Ca_{shell} ranged from 7.00 to 9.40 $\mu\text{mol mol}^{-1}$ in shell A55 (mean = 8.37 $\mu\text{mol mol}^{-1}$;
298 Fig. 3a) and from 6.91 to 11.12 $\mu\text{mol mol}^{-1}$ in shell A56 (mean = 9.23 $\mu\text{mol mol}^{-1}$; Fig. 3b).
299 Mean Li/Ca_{shell} ratio was significantly higher in shell A56 than in shell A55 (t -test $t = 16.87$,
300 $n_1 = n_2 = 332$, $p < 0.01$).

301 Annual minimum values ranged from 7.00 to 7.29 $\mu\text{mol mol}^{-1}$ in shell A55 (mean
302 [2001-2005] = 7.16 $\mu\text{mol mol}^{-1}$; $\sigma = 0.12 \mu\text{mol mol}^{-1}$), and from 7.10 to 7.64 $\mu\text{mol mol}^{-1}$ in
303 shell A56 (mean [2002-2005] = 7.44 $\mu\text{mol mol}^{-1}$; $\sigma = 0.23 \mu\text{mol mol}^{-1}$; Table 3). Mean annual
304 minima in shells A55 and A56 did not differ significantly (Mann-Whitney $U = 3$, $n_1 = 5$, $n_2 =$
305 4 , $p > 0.05$).

306 Annual maxima ranged from 9.08 to 9.40 $\mu\text{mol mol}^{-1}$ in shell A55 (mean [2001-2005] =
307 9.30 $\mu\text{mol mol}^{-1}$; $\sigma = 0.13 \mu\text{mol mol}^{-1}$), and from 10.03 to 11.12 $\mu\text{mol mol}^{-1}$ in shell A56
308 (mean [2002-2005] = 10.46 $\mu\text{mol mol}^{-1}$; $\sigma = 0.22 \mu\text{mol mol}^{-1}$; Table 3). Mean annual
309 maximum in shell A56 was significantly higher than in shell A55 (Mann-Whitney $U = 0$, $n_1 =$
310 5 , $n_2 = 4$, $p < 0.05$).

311 As a consequence, mean annual amplitude in shells A55 (2.14 $\mu\text{mol mol}^{-1}$) and A56
312 (3.02 $\mu\text{mol mol}^{-1}$) were significantly different (Mann-Whitney $U = 0$, $n_1 = 5$, $n_2 = 4$, $p < 0.05$).
313 Annual amplitude ranged from 2.01 to 2.32 $\mu\text{mol mol}^{-1}$ in shell A55, and from 2.76 to 3.63
314 $\mu\text{mol mol}^{-1}$ in shell A56 (Table 3).

315 $\text{Li}/\text{Ca}_{\text{shell}}$ in both shells was statistically correlated with the $\delta^{18}\text{O}_{\text{shell}}$ -derived temperature
316 ($p < 0.05$ for both specimens; Fig. 4). An ANCOVA showed no significant difference
317 between slopes of the two linear regressions (Bartlett's test: $B_C = 5.52$, $df = 1$; ANCOVA: $F =$
318 0.02 , $df = 1$ and 95). The strength of these correlations was, however, extremely weak with
319 determination coefficients ranging from 0.11 (shell A56) to 0.25 (shell A55). The difference
320 in intercept values (ca. 1 $\mu\text{mol mol}^{-1}$) reflects the difference in annual maxima between shell
321 A56 and shell A55.

322 The comparison of $\text{Li}/\text{Ca}_{\text{shell}}$ variations with daily shell growth rates was difficult
323 because we were unexpectedly unable to resolve microgrowth structures over the whole shell
324 sections despite etching with Mutvei's solution. Nevertheless, 22 groups of 3-5 microgrowth
325 increments were quite clearly revealed in the A56 shell portion formed in 2004. The average

326 increment width in each of these 22 batches was calculated and plotted with the A56 Li/Ca_{shell}
327 record for year 2004 (Fig. 5a). Although the number of increment data was limited, our data
328 showed that Li/Ca_{shell} covaried with microgrowth increment width, which ranged from 24-28
329 μm near the annual lines to 43 μm in the first half of the 2004 growing season (average = 32.3
330 μm). A simple linear regression indicated that microgrowth increment width explained 53%
331 of the Li/Ca_{shell} variability in shell A56 ($p < 0.001$; Fig. 5b). Note that all geochemical and
332 shell growth data obtained on specimens A55 and A56 can be retrieved in the auxiliary
333 material.

334

335 4. DISCUSSION

336

337 4.1. Seasonal timing of geochemical records in shells

338 The present study is the first to investigate Li/Ca records in bivalve shells. Li/Ca_{shell}
339 seasonal variations in our two *Arctica islandica* specimens were well-marked, presenting a
340 1.3- to 1.6-fold range over a given growing season (Fig. 3). The inter-annual variability
341 between ontogenetic ages 3 to 8 was far less pronounced than intra-annual variability.
342 Combined analyses of Li/Ca_{shell} and $\delta^{18}\text{O}_{\text{shell}}$, and reconstruction of seawater temperature from
343 $\delta^{18}\text{O}_{\text{shell}}$ allowed us to estimate the seasonal timing of Li/Ca_{shell} variations.

344 $T_{\delta^{18}\text{O}}$ variations (average annual range = 3.1 – 8.5°C) showed that the whole annual
345 range of seawater temperature (2.8 to 7.9°C at 20 m depth at LA1) was recorded by the shells
346 (Table 2). This implies that *A. islandica* shells did not stop growing because of thermal stress.
347 Conversely, the position of the annual growth breaks between minimum and maximum
348 $\delta^{18}\text{O}_{\text{shell}}$ (i.e. between maximum and minimum temperatures, recorded in August and March,
349 respectively) suggests that shells stopped growing between September and February. The
350 average microgrowth increment width measured in shell A56 was 32.3 μm at ontogenetic age

351 6, i.e. similar to the value calculated by Schöne et al. (2005a) for North Sea specimens (31.5
352 μm at ontogenetic age 4). This suggests that shell growth lasted ca. 185 days to achieve the
353 5.96 mm width of the 2004 annual increment. This result supports the hypothesis of a ca. 6-
354 month growth break between September and February. As minimum temperatures were
355 recorded by $\delta^{18}\text{O}_{\text{shell}}$, shells did not stop growing because of harsh winter conditions. Schöne
356 et al. (2005a) showed that *A. islandica* specimens from the North Sea stopped growing from
357 early September to mid-November and described this growth break as a spawning biocheck.
358 In Iceland, *A. islandica* spawning activity peaks in June-July, whereas gametogenesis occurs
359 from January to May (Thorarinsdóttir, 2000). Therefore, the annual growth breaks found in
360 our specimens cannot be attributed to reproductive activity. Moreover, our specimens were
361 likely juveniles as in Icelandic waters, only 10% of *A. islandica* of 40 mm shell length are
362 mature (Thorarinsdóttir and Jacobson, 2005). Therefore, the origin of these annual growth
363 breaks remains unclear. Their investigation, however, is far beyond the goals of this paper.
364 The most important point is that the timing of the growing season determined by $T_{\delta^{18}\text{O}}$
365 variations allowed us to conclude that $\text{Li}/\text{Ca}_{\text{shell}}$ increases from March to May, i.e. right after
366 the annual line, stays roughly stable in June, and then decreases in July–August.

367

368 **4.2. Processes potentially involved in $\text{Li}/\text{Ca}_{\text{shell}}$ seasonal variations**

369 The shape of $\text{Li}/\text{Ca}_{\text{shell}}$ variations is very similar in shells A55 and A56 and as such this
370 ratio likely responds to environmental variations or to variations of a physiological process
371 synchronized within a given population by genetic and/or exogenous factors. Based on
372 published literature on Li/Ca ratios in CaCO_3 structures, the following parameters may
373 provide plausible hypotheses to explain the $\text{Li}/\text{Ca}_{\text{shell}}$ variations in *A. islandica*: temperature,
374 calcification rate, and Li/Ca ratio in seawater. Their potential influence on the shell
375 geochemistry will be discussed in light of the evidence presented here. A fourth hypothesis

376 will also be put forward: the influence of suspended Li-rich particles originating from the
377 mechanical weathering of basaltic rocks.

378

379 4.2.1. Temperature

380 Several studies have found a significant inverse relationship between Li/Ca in CaCO₃
381 structures and temperature in coralline aragonite (Marriott et al., 2004b; Montagna et al.,
382 2006), in foraminiferal calcite (Hall and Chan, 2004; Marriott et al., 2004a), in calcitic
383 brachiopods (Delaney et al., 1989), and in inorganic calcite (Marriott et al., 2004b). We also
384 found relationships with temperature in *A. islandica* aragonitic shells but these were positive,
385 not negative (Fig. 4). Unlike these previous studies, our findings agree with thermodynamic
386 calculations predicting that Li concentration in CaCO₃ structures should decrease with
387 decreasing temperature (Hall and Chan, 2004). According to Okumura and Kitano (1986), Li
388 is incorporated in the crystal structure of aragonite in substitution of Ca, leading to the
389 formation of lithium carbonate (Li₂CO₃) crystals. Smith et al. (1971) showed that the
390 solubility of Li₂CO₃ increases with decreasing temperature. In other words, crystallization of
391 Li₂CO₃ becomes easier as temperature rises (an almost linear relationship between 0 and
392 30°C; Smith et al., 1971). Although statistically significant ($p < 0.05$), the strength of our
393 temperature-Li/Ca_{shell} relationships is extremely weak ($0.11 < r^2 < 0.25$). The weakness of this
394 relationship is particularly obvious for the 2003 Li/Ca_{shell} record in shell A56 where an
395 important offset can be seen between Li/Ca_{shell} and $\delta^{18}\text{O}_{\text{shell}}$ (Fig. 3b). Our findings suggest
396 that if temperature-dependant solubility of Li₂CO₃ really plays a role on Li/Ca_{shell} in
397 *A. islandica*, this influence is extremely weak.

398

399 4.2.2. Calcification rate

400 Many authors have suggested that the main factor controlling Li incorporation in
401 foraminiferal calcite could be calcification rate, which may itself correlate partly with
402 temperature (Delaney et al., 1985; Hall and Chan, 2004; Marriott et al, 2004a). According to
403 Carré et al. (2006), crystal growth rate strongly influences incorporation of Sr, Ba, Mn, and
404 Mg in aragonitic shells of two Peruvian bivalve species (*Mesodesma donacium* and *Chione*
405 *subrugosa*). However, they did not investigate Li/Ca_{shell} ratios. Our own results seem to
406 support these findings. Indeed, we found a relatively strong relationship between microgrowth
407 increment width and Li/Ca in *A. islandica* shells (Fig. 5). Although microgrowth increment
408 width represents the dorso-ventral linear extension of the shell per unit time and may slightly
409 differ from the absolute calcification rate (see Gillikin et al. (2005) for elaboration), our
410 results suggest that Li/Ca_{shell} may increase as a direct response of increasing calcification rate.
411 Another argument in favor of this hypothesis is the difference observed in the range of Li/Ca
412 variations in shells A55 and A56; although these two specimens appeared to have grown at an
413 equivalent annual rate from 1999 to 2006, it can be assumed that A56 reached higher daily
414 growth rates in summer than A55, explaining the difference in annual Li/Ca_{shell} maxima
415 between these two shells. The mechanisms involved in these vital effects are unknown and
416 any discussion on that subject would be highly speculative due to the scarcity of studies
417 dealing with the formation of Li₂CO₃ crystals within aragonitic structures. Identification of
418 these mechanisms would require biomineralization and/or inorganic precipitation
419 experiments.

420

421 4.2.3. Li/Ca_{seawater}

422 Delaney et al. (1985) and Hathorne and James (2006) suggested that Li/Ca ratio in
423 calcitic foraminifera was directly controlled by the Li/Ca of the growing medium. Could
424 possible variations of Li/Ca_{seawater} over *A. islandica* growing season have an influence on the

425 shell geochemistry? Li is essentially conservative in seawater with an almost constant
426 concentration of $26 \mu\text{mol L}^{-1}$ and a $\text{Li}/\text{Ca}_{\text{seawater}}$ ratio of ca. $2310 \mu\text{mol mol}^{-1}$ (Li, 2000). It has
427 no significant involvement in biological activity or scavenging by particles (Stoffyn-Egli and
428 Mackenzie, 1984). Given the long residence times of Li (1.5 million years; Huh et al., 1998)
429 and Ca (1 million year; Broecker and Peng, 1982), the Li/Ca ratio of the global ocean has
430 probably not changed over the Holocene (Hall and Chan, 2004). The two major sources of Li
431 to the ocean are (1) high-temperature basalt-seawater reactions, and (2) river input from the
432 weathering of continental crust (Hoefs and Sywall, 1997). In hydrothermal systems near the
433 mid-ocean ridges, Li is leached from oceanic basalts at temperatures $>250^{\circ}\text{C}$ (Hoefs and
434 Sywall, 1997). Although the mid-Atlantic ridge runs right through Iceland, it is unlikely that
435 such high temperatures could be reached at shallow coastal locations. Moreover, it is hardly
436 conceivable that Li leaching from this ridge would follow a seasonal pattern; it is rather
437 roughly constant throughout the year. Therefore, high-temperature hydrothermal circulation
438 can certainly not explain $\text{Li}/\text{Ca}_{\text{shell}}$ seasonal variations.

439 Seasonal variations of riverine inputs may, however, have a local influence on Li/Ca
440 ratios in coastal waters. Intensities of chemical and mechanical weathering of silicate rocks
441 like basalts are usually expressed in terms of fluxes of dissolved and suspended materials,
442 respectively (Gislason et al., 2009). Gislason et al. (2009) found a relationship between air
443 temperature and chemical weathering rate in 8 northeastern Iceland river catchments. Air
444 temperature in Iceland starts increasing in March and reaches maxima in July. Intensity of
445 chemical weathering may therefore follow the same general pattern as $\text{Li}/\text{Ca}_{\text{shell}}$. Pogge von
446 Strandmann et al. (2006) analyzed the chemical composition of 25 Icelandic rivers in
447 September 2003 and August 2005 and found an average dissolved Li concentration of 87.5
448 nmol L^{-1} (range: $1.54\text{--}1250 \text{ nmol L}^{-1}$) and a $\text{Li}/\text{Ca}_{\text{river}}$ ratio ranging from 31 to $2461 \mu\text{mol}$
449 mol^{-1} (average = $563 \mu\text{mol mol}^{-1}$). This dissolved Li concentration range is similar to that

450 measured by Vigier et al. (2009) in the major Icelandic rivers (range: 3–317 nmol L⁻¹; average
451 = 86.5 nmol L⁻¹). These values may be slightly higher in July, ie. at the annual air temperature
452 maximum. According to Delaney et al. (1985), a 1.8 to 2.6-fold increase of the average
453 Li/Ca_{seawater} ratio is necessary to observe a 1.3 to 1.6-fold increase of Li/Ca in calcitic
454 foraminifera. This relationship can probably not be applied to *A. islandica* shells because of
455 their aragonitic structure. Nevertheless, it highlights that Li/Ca_{seawater} must increase
456 significantly to induce a 1.3 to 1.6-fold increase of Li/Ca in biogenic carbonates. Given that
457 the maximum Li/Ca_{river} ratio measured by Pogge von Strandmann et al. (2006) was only 1.1-
458 fold higher than Li/Ca_{seawater}, seasonal variations of basalt chemical weathering and dissolved
459 Li flux can hardly explain the full variability of Li/Ca_{shell} in *A. islandica*.

460

461 4.2.4. Suspended Li-rich basaltic particles

462 A fourth hypothesis could be put forward to explain Li/Ca_{shell} seasonal variations: the
463 possible influence of weathered basaltic particles carried by rivers. Seasonal variations of
464 Sandá River discharge were obtained from the Hydrological Service of the Icelandic National
465 Energy Authority (<http://www.os.is/>; Fig. 6). These data show that discharge roughly follows
466 the same seasonal pattern as Li/Ca_{shell}, with values ranging from ca. 10 m³ s⁻¹ in fall and
467 winter to ca. 35 m³ s⁻¹ in June (long term average). Could these variations in river discharge
468 induce large changes in the flux of suspended particles? Gislason et al. (2009) described and
469 quantified a direct relationship between river discharge and mechanical weathering (expressed
470 as suspended inorganic material (SIM) flux) in 8 river catchments in northeast Iceland.
471 Depending on which of their 8 discharge-SIM flux equations is used for calculation, the 350%
472 seasonal increase in river discharge would induce a 350 to 4900% increase in SIM flux over a
473 year. Therefore, high loads of suspended basaltic particles probably flow to the sea with
474 Icelandic rivers as soon as the snow melts, reaching a peak roughly at the same time as the

475 Li/Ca_{shell} annual maximum. These river particles have a high Li content (several ppm; Pogge
476 von Strandmann et al., 2006), ca. 1 order of magnitude larger than in shells. Although the
477 freshwater inputs likely flow as a thin surface layer (ca. 10 meters thickness; cf. Assthorsson,
478 1990; Andrews et al., 2001), it is likely that suspended material carried by rivers can cross the
479 halocline and settle on the seafloor, thus modifying the chemistry of bottom waters.
480 Consequently, these Li-rich particles may significantly increase Li/Ca_{shell}, either directly (if
481 ingested, transferred to the internal fluids, and then incorporated within the shell during
482 biomineralization) or indirectly if they weather after deposition on the seafloor. This
483 hypothesis could be tested in further studies through analyses of the lithium isotope
484 composition of *A. islandica* shells. SIM originating from the weathering of basaltic material
485 has a very low $\delta^7\text{Li}$ value ($\delta^7\text{Li}_{\text{SIM}} = -1.3$ to 7.5% in Icelandic rivers; Pogge von Strandmann
486 et al., 2006) in comparison to seawater ($\delta^7\text{Li}_{\text{seawater}} = 32\%$; Huh et al., 1998). If indeed Li
487 incorporation in shells is linked to Li-rich particle inputs by rivers, then shell aragonite must
488 have a $\delta^7\text{Li}$ several per mil lighter than seawater.

489

490 4.3. Conclusions

491 Lithium is likely incorporated in *A. islandica* aragonitic shells as lithium carbonate
492 Li_2CO_3 , i.e. Li^+ substitutes for Ca^{2+} at the site of calcification in the extrapallial fluid. Several
493 explanations could account for the observed seasonal variations in Li/Ca ratio in shells:

494 1 - The significant positive relationship found between $\delta^{18}\text{O}_{\text{shell}}$ -derived temperature and
495 Li/Ca_{shell} suggests that seasonal Li/Ca_{shell} variations could be linked to increasing solubility of
496 Li_2CO_3 with decreasing temperature in the extrapallial fluid. However, the strength of this
497 relationship is so weak that temperature-dependant solubility of Li_2CO_3 cannot possibly be
498 the main factor controlling Li/Ca_{shell} variations;

499 2 - Given the strong and significant positive relationship found between $\text{Li}/\text{Ca}_{\text{shell}}$ and
500 microgrowth increment width, $\text{Li}/\text{Ca}_{\text{shell}}$ may partly be controlled by variations in calcification
501 rate. As this rate is also partly controlled by temperature, it is difficult to make conclusions
502 about the exact importance of Li_2CO_3 solubility in $\text{Li}/\text{Ca}_{\text{shell}}$ variations;

503 3 - Sandá river discharge and $\text{Li}/\text{Ca}_{\text{shell}}$ presented an intriguing similarity in their seasonal
504 variations. As soon as snow melts in spring, mechanical weathering of basaltic rocks gains
505 intensity due to the increased river discharge, leading to a massive flow of Li-rich silicate
506 particles into the ocean. This phenomenon reaches a peak at the same time as $\text{Li}/\text{Ca}_{\text{shell}}$. We
507 therefore suggest that this massive input of Li could be trapped in the shell, thus impacting
508 $\text{Li}/\text{Ca}_{\text{shell}}$.

509 If indeed $\text{Li}/\text{Ca}_{\text{shell}}$ is mainly controlled by calcification rate, then this ratio may be
510 useful to address seasonal variations in growth rate of bivalve species in which daily growth
511 increments and lines are not easily discernable. In turn, abrupt decreases of $\text{Li}/\text{Ca}_{\text{shell}}$ may be
512 helpful to identify growth retardations, for instance related to the occurrence of toxic
513 phytoplankton blooms in coastal ecosystems. Alternatively, if $\text{Li}/\text{Ca}_{\text{shell}}$ in *A. islandica* is
514 controlled by river inputs of Li-rich silicate particles, it may then be used a proxy for the
515 intensity of mechanical weathering of Icelandic basaltic rocks. This could have exciting
516 perspectives, e.g. to get a better insight about the frequency and intensity of past jökulhlaups
517 (subglacial outburst floods). It may also be interesting to analyze the geochemical
518 composition of recent *A. islandica* shells from the south-east coast of Iceland, where a huge
519 jökulhlaup flowed under the Vatnajökull glacier in 1996 because of the subglacial eruption of
520 the Grímsvötn Volcano. In any event, it is clear from our work that further studies, including
521 $\delta^7\text{Li}_{\text{shell}}$ analyses and experiments under controlled conditions, are needed to better understand
522 $\text{Li}/\text{Ca}_{\text{shell}}$ variations in bivalve shells and to determine if this could be a useful proxy for
523 paleoecological reconstructions.

524
525
526
527
528
529
530
531
532
533
534
535
536
537
538
539
540
541
542

ACKNOWLEDGMENTS

We acknowledge Jens Fiebig (University of Frankfurt, Germany) for isotopic analyses of *Arctica* shells, Chris Romanek (University of Georgia, USA) for $\delta^{18}\text{O}$ analysis of water samples, and Sven Baier for help during dredging in Iceland. Dredging of samples was kindly made possible through Siggeir Stefánsson and Þorgrímur Kjartansson (Hraðfrystistöð Þórshafnar, Iceland). We also express deep appreciation to the Oceanographic Group of the Marine Research Institute of Reykjavik for making their temperature and salinity data freely available on their website (<http://www.hafro.is/Sjora/>), and to the Hydrological Service of the Icelandic National Energy Authority for Sandá River discharge data (data available at <http://www.os.is/>). Thanks are due to the NASA Goddard Institute for Space Studies and especially Gavin Schmidt, Grant Bigg and Eelco Rohling for their compilation of salinity and $\delta^{18}\text{O}_{\text{water}}$ data (<http://data.giss.nasa.gov/o18data/>), and to the scientists of the VEINS Program who made their salinity and $\delta^{18}\text{O}_{\text{water}}$ data available on the NASA website. This manuscript has greatly benefited from critical reviews and very helpful comments by Katie Matthews and two anonymous reviewers. Financial support for this study was provided by the German Research Foundation (DFG) to Bernd R. Schöne (SCHO 793/4). Julien Thébaud gratefully acknowledges the Alexander von Humboldt Foundation (Bonn, Germany) for the award of a Research Fellowship for Postdoctoral Researchers. This is Geocycles publication number 627.

543
544
545
546
547
548
549
550
551
552
553
554
555
556
557
558
559
560
561
562
563
564
565
566
567**REFERENCES**

- Andrews, J. T., C. Caseldine, N. J. Weiner, and J. Hatton (2001), Late Holocene (ca. 4 ka) marine and terrestrial environmental change in Reykjarfjörður, north Iceland: climate and/or settlement?, *J. Quarter. Sci.*, *16*, 133-143.
- Astthorsson, O. S. (1990), Ecology of the euphausiids *Thysanoessa raschi*, *T. inermis* and *Meganyctiphanes norvegica* in Ísafjord-deep, northwest-Iceland, *Mar. Biol.*, *107*, 147-157.
- Broecker, W. S., and T.-H. Peng (Eds.) (1982), *Tracers in the sea*, 690 pp., Eldigio Press, Palisades.
- Carré, M., I. Bentaleb, O. Bruguier, E. Ordinola, N. T. Barrett, and M. Fontugne (2006), Calcification rate influence on trace element concentrations in aragonitic bivalve shells: Evidences and mechanisms, *Geochim. Cosmochim. Acta*, *70*, 4906-4920.
- Carriker, M. R., C. P. Swann, J. Ewart, and C. L. Counts III (1996), Ontogenetic trends of elements (Na to Sr) in prismatic shell of living *Crassostrea virginica* (Gmelin) grown in three ecologically dissimilar habitats for 28 weeks: a proton probe study, *J. Exp. Mar. Biol. Ecol.*, *201*, 87-135.
- Chauvaud, L., A. Lorrain, R. B. Dunbar, Y.-M. Paulet, G. Thouzeau, F. Jean, J.-M. Guarini, and D. Mucciarone (2005), Shell of the Great Scallop *Pecten maximus* as a high-frequency archive of paleoenvironmental changes, *Geochem. Geophys. Geosystems*, *6*(8), Q08001, doi:10.1029/2004GC000890.
- Craig, C.-A., K. E. Jarvis, and L. J. Clarke (2000), An assessment of calibration strategies for the quantitative and semi-quantitative analysis of calcium carbonate matrices by laser ablation-inductively coupled plasma-mass spectrometry (LA-ICP-MS), *J. Anal. At. Spectrom.*, *15*, 1001-1008.

- 568 Delaney, M. L., A. W. H. Bé, and E. A. Boyle (1985), Li, Sr, Mg, and Na in foraminiferal
569 calcite shells from laboratory culture, sediment traps, and sediment cores, *Geochim.*
570 *Cosmochim. Acta*, *49*, 1327-1341.
- 571 Delaney, M. L., B. N. Popp, C. G. Lepzelter, and T. F. Anderson (1989), Lithium-to-calcium
572 ratios in modern, Cenozoic, and Paleozoic articulate brachiopod shells,
573 *Paleoceanography*, *4*, 681-691.
- 574 Dick, D., E. Philipp, M. Kriews, and D. Abele (2007), Is the umbo matrix of bivalve shells
575 (*Laternula elliptica*) a climate archive?, *Aquat. Toxicol.*, *84*, 450-456.
- 576 Epplé, V. M. (2004), High-resolution climate reconstruction for the Holocene based on
577 growth chronologies of the bivalve *Arctica islandica* from the North Sea, Ph.D. thesis,
578 101 pp., University of Bremen, 17 December.
- 579 Epstein, S., R. Buchsbaum, H. A. Lowenstam, and H. C. Urey (1953), Revised carbonate-
580 water isotopic temperature scale, *Bull. Geol. Soc. Am.*, *64*, 1315-1326.
- 581 Fiebig, J., B. R. Schöne, and W. Oschmann (2005), High-precision oxygen and carbon
582 isotope analysis of very small (10–30 µg) amounts of carbonates using continuous flow
583 isotope ratio mass spectrometry, *Rapid Commun. Mass Spectrom.*, *19*, 2355-2358.
- 584 Gillikin, D. P., A. Lorrain, J. Navez, J. W. Taylor, L. André, E. Keppens, W. Baeyens, and F.
585 Dehairs (2005), Strong biological controls on Sr/Ca ratios in aragonitic marine bivalve
586 shells, *Geochem. Geophys. Geosystems*, *6*(5), Q05009, doi:10.1029/2004GC000874.
- 587 Gislason, S. R., et al. (2009), Direct evidence of the feedback between climate and
588 weathering, *Earth and Planetary Science Letters*, *277*, 213-222.
- 589 Grossman, E. L., and T.-L. Ku (1986), Oxygen and carbon isotope fractionation in biogenic
590 aragonite; temperature effects, *Chem. Geol.*, *59*, 59-74.

- 591 Hall, J. M., and L.-H. Chan (2004), Li/Ca in multiple species of benthic and planktonic
592 foraminifera: thermocline, latitudinal, and glacial-interglacial variation, *Geochim.*
593 *Cosmochim. Acta*, *68*, 529-545.
- 594 Hathorne, E. C., and R. H. James (2006), Temporal record of lithium in seawater: A tracer for
595 silicate weathering?, *Earth Planet. Sci. Lett.*, *246*, 393-406.
- 596 Henderson, G. M. (2002), New oceanic proxies for paleoclimate, *Earth Planet. Sci. Lett.*, *203*,
597 1-13.
- 598 Hoefs, J., and M. Sywall (1997), Lithium isotope composition of quaternary and tertiary
599 biogene carbonates and a global lithium isotope balance, *Geochim. Cosmochim. Acta*,
600 *61*, 2679-2690.
- 601 Hopkins, T. S. (1991), The GIN Sea - a synthesis of its physical oceanography and literature
602 review 1972-1985, *Earth Sci. Rev.*, *30*, 175-318.
- 603 Huh, Y., L.-H. Chan, L. Zhang, and J. M. Edmond (1998), Lithium and its isotopes in major
604 world rivers: implications for weathering and the oceanic budget, *Geochim. Cosmochim.*
605 *Acta*, *62*, 2039-2051.
- 606 Hut, G. (1987), Consultants' group meeting on stable isotope reference samples for
607 geochemical and hydrological investigations, *Report to the Director General*, 44 pp.,
608 International Atomic Energy Agency, Vienna.
- 609 Jones, D. S. (1983), Sclerochronology: Reading the record of the molluscan shell, *Am. Sci.*,
610 *71*, 384-391.
- 611 Jones, D. S. (1998), Isotopic determination of growth and longevity on fossil and modern
612 invertebrates, *Palaeontol. Soc. Pap.*, *4*, 37-67.
- 613 Kilada, R. W., S. E. Campana, and D. Roddick (2007), Validated age, growth, and mortality
614 estimates of the ocean quahog (*Arctica islandica*) in the western Atlantic, *ICES J. Mar.*
615 *Sci.*, *64*, 31-38.

- 616 Kurosawa, M., S. E. Jackson, and S. Sueno (2002), Trace element analysis of NIST SRM 614
617 and 616 glass reference materials by Laser Ablation Microprobe-Inductively Coupled
618 Plasma-Mass Spectrometry, *Geostand. Geoanal. Res.*, *26*, 75-84.
- 619 Li, Y.-H. (Ed.) (2000), *A compendium of geochemistry: From solar nebula to the human*
620 *brain*, 440 pp., Princeton University Press, Princeton.
- 621 Liehr, G. A., M. L. Zettler, T. Leipe, and G. Witt (2005), The ocean quahog *Arctica islandica*
622 L.: a bioindicator for contaminated sediments, *Mar. Biol.*, *147*, 671-679.
- 623 Lindh, U., H. Mutvei, T. Sunde, and T. Westermark (1988), Environmental history told by
624 mussel shells, *Nucl. Instr. Meth. Phys. Res. B*, *30*, 388-392.
- 625 Lingard, S. M., R. D. Evans, and B. P. Bourgoin (1992), Method for the estimation of
626 organic-bound and crystal-bound metal concentrations in bivalve shells, *Bull. Environ.*
627 *Contam. Toxicol.*, *48*, 179-184.
- 628 Longerich, H. P., S. E. Jackson, and D. Günther (1996), Laser ablation inductively coupled
629 plasma mass spectrometric transient signal data acquisition and analyte concentration
630 calculation, *J. Anal. At. Spectrom.*, *11*, 899-904.
- 631 Marchitto, T. M., G. A. Jones, G. A. Goodfriend, and C. R. Weidman (2000), Precise
632 temporal correlation of Holocene mollusk shells using sclérochronologie, *Quat. Res.*,
633 *53*, 236-246.
- 634 Marin, F., and G. Luquet (2004), Molluscan shell proteins, *C. R. Palevol*, *3*, 469-492.
- 635 Marriott, C. S., G. M. Henderson, R. Crompton, M. Staubwasser, and S. Shaw (2004a), Effect
636 of mineralogy, salinity, and temperature on Li/Ca and Li isotope composition of calcium
637 carbonate, *Chem. Geol.*, *212*, 5-15.
- 638 Marriott, C. S., G. M. Henderson, N. S. Belshaw, and A. W. Tudhope (2004b), Temperature
639 dependence of $\delta^7\text{Li}$, $\delta^{44}\text{Ca}$ and Li/Ca during growth of calcium carbonate, *Earth Planet.*
640 *Sci. Lett.*, *222*, 615-624.

- 641 McCrea, J. M. (1950), On the isotopic chemistry of carbonates and a paleotemperature scale,
642 *J. Chem. Phys.*, *18*, 849-857.
- 643 Montagna, P., M. McCulloch, C. Mazzoli, S. Silenzi, and S. Schiaparelli (2006), Li/Ca ratios
644 in the Mediterranean non-tropical coral *Cladocora caespitosa* as a potential
645 paleothermometer, *Geophys. Res. Abstr.*, *8*, Abstract 03695.
- 646 Okumura, M., and Y. Kitano (1986), Coprecipitation of alkali metal ions with calcium
647 carbonate, *Geochim. Cosmochim. Acta*, *50*, 49-58.
- 648 Pannella, G., and C. McClintock (1968), Biological and environmental rhythms reflected in
649 molluscan shell growth, *J. Paleontol.*, *42*, 64-80.
- 650 Pearce, N. J. G., W. T. Perkins, J. A. Westgate, M. P. Gorton, S. E. Jackson, C. R. Neal, and
651 S. P. Chenery (1997), A compilation of new and published major and trace element data
652 for NIST SRM 610 and NIST SRM 612 glass reference materials, *Geostand. Geoanal.*
653 *Res.*, *21*, 115-144.
- 654 Pogge von Strandmann, P. A. E., K. W. Burton, R. H. James, P. van Calsteren, S. R. Gíslason,
655 and F. Mokadem (2006), Riverine behaviour of uranium and lithium isotopes in an
656 actively glaciated basaltic terrain, *Earth Planet. Sci. Lett.*, *251*, 134-147.
- 657 Scherrer, B. (1984), *Biostatistiques*, 850 pp., Gaëtan Morin Editeur, Québec.
- 658 Schmidt, G.A., G. R. Bigg, and E. J. Rohling (1999), Global seawater oxygen-18 database,
659 <http://data.giss.nasa.gov/o18data/>, Goddard Institute for Space Studies, New York.
- 660 Schöne, B. R. (2008), The curse of physiology—challenges and opportunities in the
661 interpretation of geochemical data from mollusk shells, *Geo-Marine Lett.*, *28*, 269-285.
- 662 Schöne, B. R., W. Oschmann, J. Rössler, A. D. Freyre Castro, S. D. Houk, I. Kröncke, W.
663 Dreyer, R. Janssen, H. Rumohr, and E. Dunca (2003), North Atlantic Oscillation
664 dynamics recorded in shells of a long-lived bivalve mollusk, *Geology*, *31*, 1037-1040.

- 665 Schöne, B. R., A. D. Freyre Castro, J. Fiebig, S. D. Houk, W. Oschmann, and I. Kröncke
666 (2004), Sea surface water temperatures over the period 1884–1983 reconstructed from
667 oxygen isotope ratios of a bivalve mollusk shell (*Arctica islandica*, southern North Sea),
668 *Palaeogeogr. Palaeoclimatol. Palaeoecol.*, *212*, 215-232.
- 669 Schöne, B. R., S. D. Houk, A. D. Freyre Castro, J. Fiebig, W. Oschmann, I. Kröncke, W.
670 Dreyer, and F. Gosselck (2005a), Daily growth rates in shells of *Arctica islandica*:
671 Assessing sub-seasonal environmental controls on a long-lived bivalve mollusk,
672 *Palaios*, *20*, 78-92.
- 673 Schöne, B. R., J. Fiebig, M. Pfeiffer, R. Gleß, J. Hickson, A. L. A. Johnson, W. Dreyer, and
674 W. Oschmann (2005b), Climate records from a bivalved Methuselah (*Arctica islandica*,
675 Mollusca; Iceland), *Palaeogeogr. Palaeoclimatol. Palaeoecol.*, *228*, 130-148.
- 676 Schöne, B. R., M. Pfeiffer, T. Pohlmann, and F. Siegismund (2005c), A seasonally resolved
677 bottom-water temperature record for the period AD 1866-2002 based on shells of
678 *Arctica islandica* (Mollusca, North Sea), *Int. J. Climatol.*, *25*, 947-962.
- 679 Schöne, B. R., E. Dunca, J. Fiebig, and M. Pfeiffer (2005d), Mutvei's solution: An ideal agent
680 for resolving microgrowth structures of biogenic carbonates, *Palaeogeogr.*
681 *Palaeoclimatol. Palaeoecol.*, *228*, 149-166.
- 682 Smith, S. H., D. D. Williams, and R. R. Miller (1971), Solubility of lithium carbonate at
683 elevated temperatures, *J. Chem. Eng. Data*, *16*, 74-75.
- 684 Stecher III, H. A., D. E. Krantz, C. J. Lord III, G. W. Luther III, and K. W. Bock (1996),
685 Profiles of strontium and barium in *Mercenaria mercenaria* and *Spisula solidissima*
686 shells, *Geochim. Cosmochim. Acta*, *60*, 3445-3456.
- 687 Stoffyn-Egli, P., and F. T. Mackenzie (1984), Mass balance of dissolved lithium in the
688 oceans, *Geochim. Cosmochim. Acta*, *48*, 859-872.

- 689 Thébault, J., L. Chauvaud, J. Clavier, J. Guarini, R. B. Dunbar, R. Fichez, D. A. Mucciarone,
690 and E. Morize (2007), Reconstruction of seasonal temperature variability in the tropical
691 Pacific Ocean from the shell of the scallop, *Comptopallium radula*. *Geochim.*
692 *Cosmochim. Acta*, *71*, 918-928.
- 693 Thébault, J., L. Chauvaud, S. L'Helguen, J. Clavier, A. Barats, S. Jacquet, C. Pécheyran, and
694 D. Amouroux (2009), Barium and molybdenum records in bivalve shells: geochemical
695 proxies for phytoplankton dynamics in coastal environments?, *Limnol. Oceanogr.*, *54*,
696 1002-1014.
- 697 Thorarinsdóttir, G. G. (2000), Annual gametogenic cycle in ocean quahog, *Arctica islandica*
698 from north-western Iceland, *J. Mar. Biol. Assoc. U. K.*, *80*, 661-666.
- 699 Thorarinsdóttir, G. G., and L. D. Jacobson (2005), Fishery biology and biological reference
700 points for management of ocean quahogs (*Arctica islandica*) off Iceland, *Fish. Res.*, *75*,
701 97-106.
- 702 Toland, H., B. Perkins, N. Pearce, F. Keenan, and M. J. Leng (2000), A study of
703 sclerochronology by laser ablation ICP-MS, *J. Anal. At. Spectrom.*, *15*, 1143-1148.
- 704 Van Achterbergh, E., C. G. Ryan, S. E. Jackson, and W. L. Griffin (2001), Data reduction
705 software for LA-ICP-MS, in *Laser ablation-ICPMS in the earth sciences: principles*
706 *and applications*, edited by P. J. Sylvester, pp. 239-243, Mineralogical Association of
707 Canada Short Course Series 29, Ottawa.
- 708 Vander Putten, E., F. Dehairs, E. Keppens, and W. Baeyens (2000), High resolution
709 distribution of trace elements in the calcite shell layer of modern *Mytilus edulis*:
710 environmental and biological controls, *Geochim. Cosmochim. Acta*, *64*, 997-1011.
- 711 Vigier, N., S. R. Gislason, K. W. Burton, R. Millot, and F. Mokadem (2009), The relationship
712 between riverine lithium isotope composition and silicate weathering rates in Iceland,
713 *Earth Planet. Sci. Lett.*, doi: 10.1016/j.epsl.2009.08.026.

- 714 Wanamaker, A. D., J. Heinemeier, J. D. Scourse, C. A. Richardson, P. G. Butler, J. Eiríksson,
715 and K. L. Knudsen (2008a), Very-long lived molluscs confirm 17th century AD tephra-
716 based radiocarbon reservoir ages for north Icelandic shelf waters, *Radiocarbon*, *50*, 399-
717 412.
- 718 Wanamaker, A. D., K. J. Kreutz, B. R. Schöne, N. Pettigrew, H. W. Borns, D. S. Introne, D.
719 Belknap, K. A. Maasch, and S. Feindel (2008b), Coupled North Atlantic slope water
720 forcing on Gulf of Maine temperatures over the past millennium, *Clim. Dyn.*, *31*, 183-
721 194.
- 722 Wefer, G., W. H. Berger, J. Bijma, and G. Fischer (1999), Clues to ocean history: a brief
723 overview of proxies, in *Use of proxies in paleoceanography: examples from the South*
724 *Atlantic*, edited by G. Fischer and G. Wefer, pp. 1-68, Springer-Verlag, Berlin.
- 725 Weidman, C. R., G. A. Jones, and K. C. Lohmann (1994), The long-lived mollusc *Arctica*
726 *islandica*: A new paleoceanographic tool for the reconstruction of bottom temperatures
727 for the continental shelves of the northern North Atlantic Ocean, *J. Geophys. Res.*, *99*,
728 18305-18314.
- 729 Witbaard, R. (1997), Tree of the sea: The use of the internal growth lines in the shell of
730 *Arctica islandica* (Bivalvia, Mollusca) for the retrospective assessment of marine
731 environmental change, Ph.D. thesis, 157 pp., Rijksuniversiteit Groningen, 30 May.
732

733

TABLES

734

735 Table 1. LA-ICP-MS operating conditions.

736

Laser: New Wave Research UP-213		ICP-MS: Agilent 7500ce	
Crystal	Nd:YAG	RF power	1200 W
Wavelength	213 nm	Plasma gas flow	15 L min ⁻¹
Laser mode	Q-switched	Auxiliary gas flow	1 L min ⁻¹
Laser power	0.2 mJ	Carrier gas flow	0.65 L min ⁻¹
Repetition rate	10 Hz	Optional gas flow	75% He
Pit diameter	80 μm	Acquisition mode	Pulse counting
Ablation time	60 s	Acquisition time	120 s
Background	60 s	Dwell time	10 ms

737

738 Table 2. Annual amplitudes of $\delta^{18}\text{O}_{\text{shell}}$ and $T_{\delta^{18}\text{O}}$ of specimens A55 and A56 over the period
 739 2002-2006. $T_{\delta^{18}\text{O}}$ were calculated using Eq. (1) using a mean $\delta^{18}\text{O}_{\text{water}}$ value of -0.55‰ . The
 740 uncertainty in temperature reconstruction from $\delta^{18}\text{O}_{\text{shell}}$ is $\pm 0.95\text{ °C}$.

741

Year	Shell	$\delta^{18}\text{O}_{\text{shell}}$ (‰VPDB)		$T_{\delta^{18}\text{O}}$ ($\pm 0.95\text{°C}$)	
		Min.	Max.	Min.	Max.
2002	A55	2.12	3.51	1.8	7.8
	A56	2.08	3.23	3.0	8.0
2003	A55	2.06	3.29	2.8	8.1
	A56	1.93	2.92	4.4	8.7
2004	A55	2.15	3.46	2.0	7.7
	A56	1.73	3.21	3.1	9.5
2005	A55	1.64	3.05	3.8	9.9
	A56	1.96	3.45	2.1	8.5
2006	A55	-	2.92	4.4	-
	A56	-	2.98	4.1	-

742

743 Table 3. Annual minima, maxima, and amplitude of $\text{Li}/\text{Ca}_{\text{shell}}$ values of specimens A55 and
744 A56 over the period 2001-2005.

745

Year	Shell	Min. $\text{Li}/\text{Ca}_{\text{shell}}$	Max. $\text{Li}/\text{Ca}_{\text{shell}}$	Annual amplitude
2001	A55	7.26	9.40	2.13
	A56	-	-	-
2002	A55	7.29	9.29	2.01
	A56	7.64	10.42	2.77
2003	A55	7.00	9.08	2.08
	A56	7.50	10.26	2.76
2004	A55	7.08	9.39	2.32
	A56	7.10	10.03	2.92
2005	A55	7.15	9.30	2.15
	A56	7.50	11.12	3.63

746

747

748

749
750
751
752
753
754
755
756
757
758
759
760
761
762
763
764
765
766
767
768
769
770
771
772**FIGURE CAPTIONS**

Fig. 1. Map of northeastern Iceland showing Langanes Peninsula between Þistilfjörður and Bakkaflói. *Arctica islandica* specimens were collected by dredging in Þistilfjörður at 30 m water-depth (black dot). Temperature and salinity data used in this paper were measured off Langanes Peninsula by the Marine Research Institute of Reykjavik (CTD station LA1, 20 m water depth, black cross). Seasonality of freshwater inputs in Þistilfjörður were assessed using river discharge data collected at Sandá River gauging station (black square).

Fig. 2. Preparation of *Arctica islandica* shells for geochemical analyses. a) Right valve of *Arctica islandica*. The axis of maximum growth was identified on shells as the largest distance between the umbo and the ventral margin (dashed line). b) After mounting on a Plexiglas cube and embedding in metal-epoxy resin, left valves were cut along the axis of maximum growth using a low-speed saw. c) Two “mirroring” sections were cut in each shell, one for isotopic analyses (thick section “A”) and the other one for Li/Ca determination (thick section “B”).

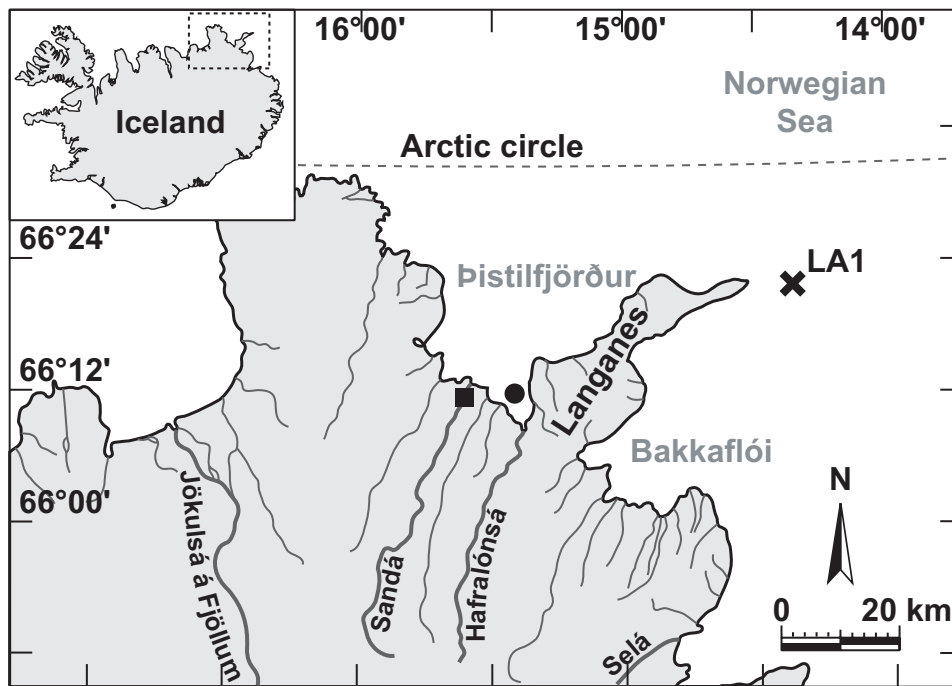
Fig. 3. Temporal variations (2000-2006) of Li/Ca_{shell} ratio (grey circles), $\delta^{18}\text{O}_{\text{shell}}$ (black triangles; inverted scale), and $\delta^{18}\text{O}_{\text{shell}}$ -derived seawater temperature ($T_{\delta^{18}\text{O}}$, grey area) measured in *Arctica islandica* shells. a) Specimen A55. b) Specimen A56. Error bars on the left side of each panel correspond to $\text{Li/Ca}_{\text{min.}} \pm 1\text{RSD}$, $\text{Li/Ca}_{\text{mean}} \pm 1\text{RSD}$, and $\text{Li/Ca}_{\text{max.}} \pm 1\text{RSD}$, with $\text{RSD} = 1.9\%$ (precision given by 22 measurements of NIST SRM 614). Vertical dashed lines represent the annual growth lines revealed in shell cross-sections, and are used to identify the different years of growth. Also presented are digitized cross-sections of the two specimens, showing annual growth lines in outer and inner shell layers, and location of aragonite samples taken for isotopic and elemental analyses.

773 Fig. 4. Correlations between $\delta^{18}\text{O}_{\text{shell}}$ -derived seawater temperature ($T_{\delta^{18}\text{O}}$) and $\text{Li}/\text{Ca}_{\text{shell}}$
774 ratio in shells A55 ($n = 48$) and A56 ($n = 50$).

775 Fig. 5. a) $\text{Li}/\text{Ca}_{\text{shell}}$ profile (grey circles) and microgrowth increment width (black
776 circles) measured during the 2004 growing season in shell A56. b) Simple linear regression
777 performed between $\text{Li}/\text{Ca}_{\text{shell}}$ and microgrowth increment width in shell A56 ($n = 22$).

778 Fig. 6. Long term smoothed daily averages of Sandá River discharge (data obtained
779 from the Hydrological Service of the Icelandic National Energy Authority). Maximum
780 discharge is recorded in May and June, i.e. in the middle of *A. islandica* shell growth season.

Figure 1



hal-00449411, version 1 - 21 Jan 2010

Figure 2

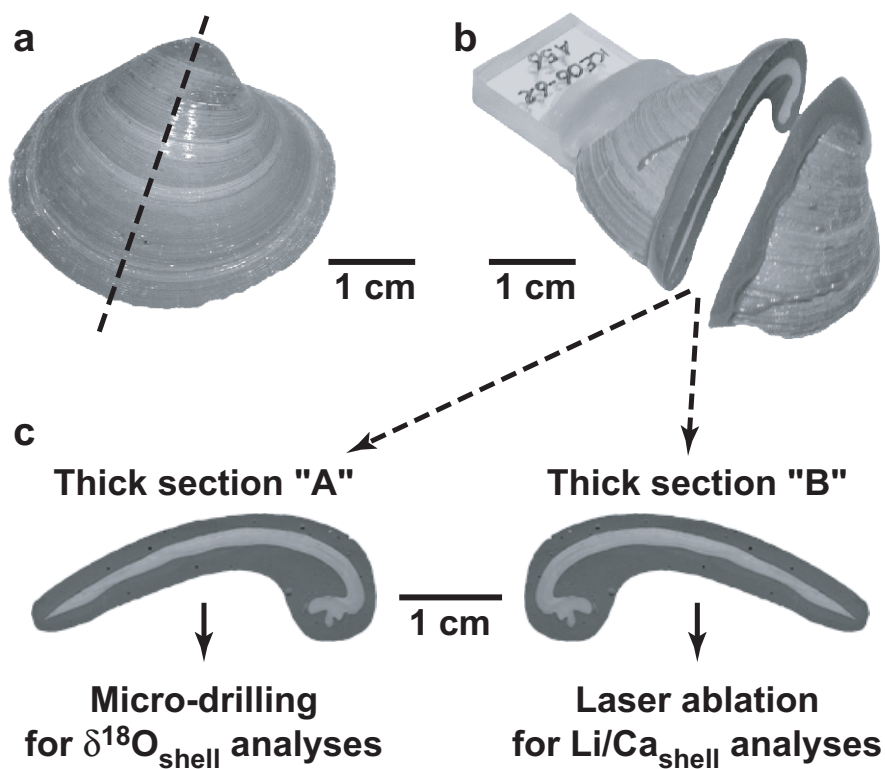
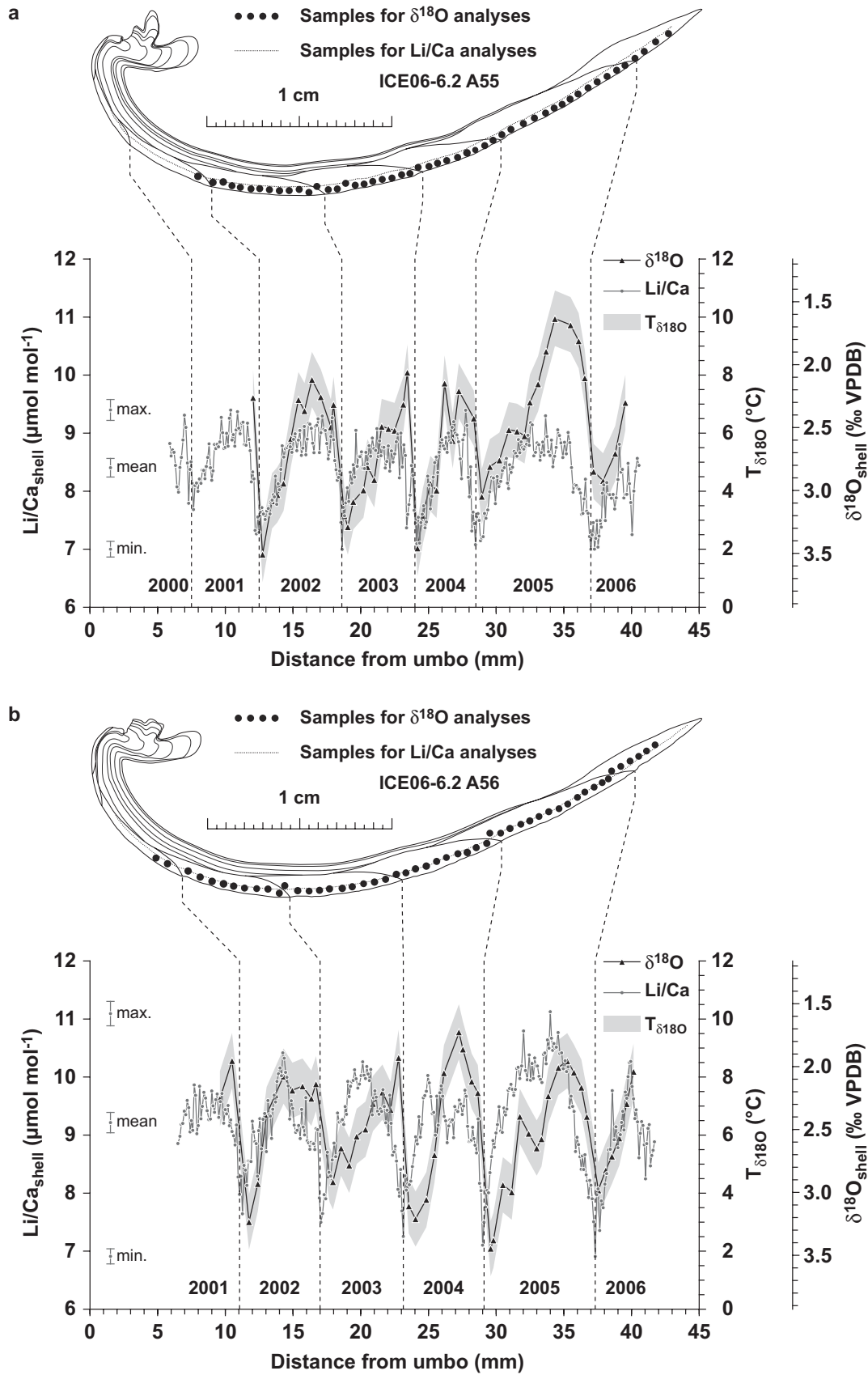


Figure 3



hal-00449411, version 1 - 21 Jan 2010

Figure 4

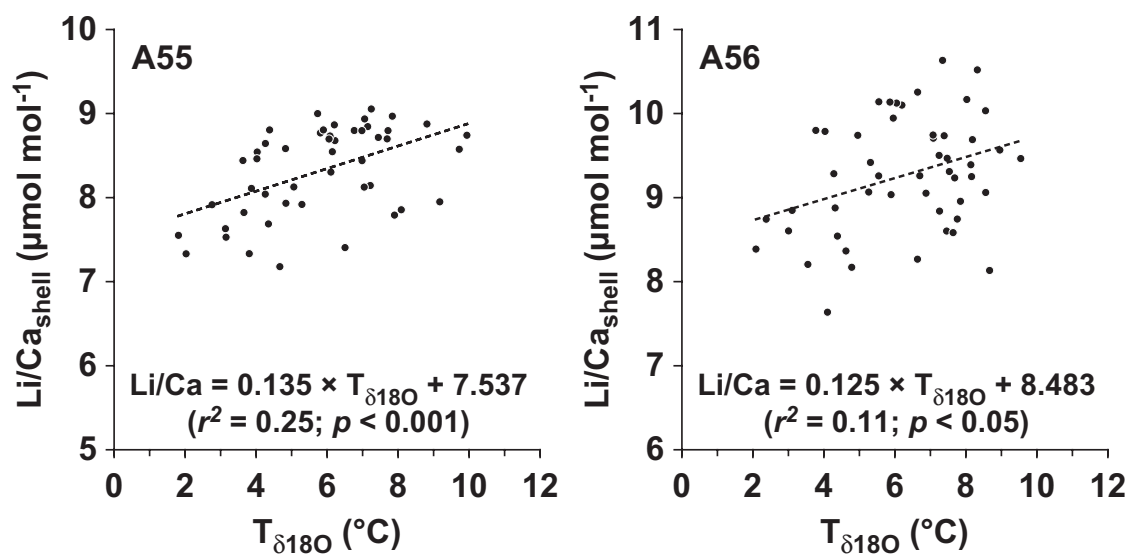


Figure 5

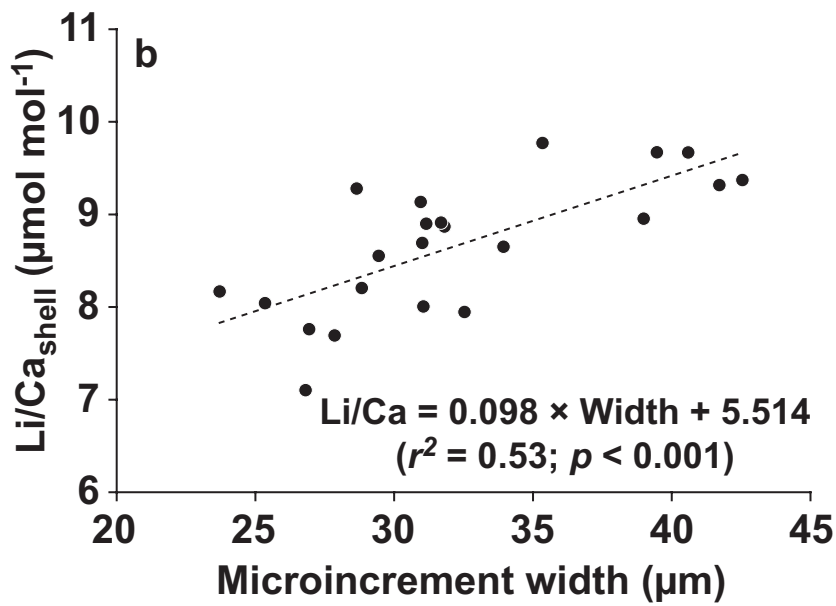
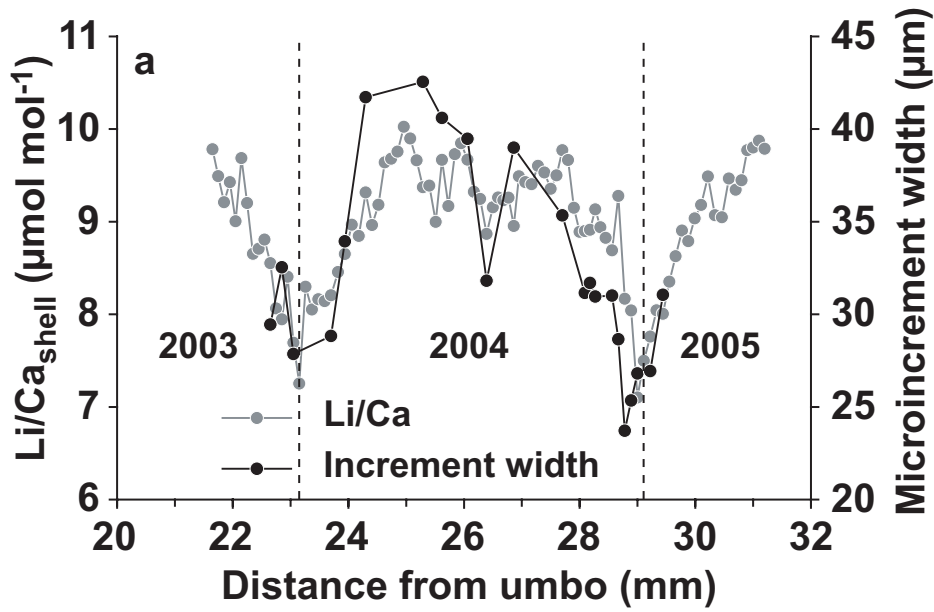


Figure 6

